2008 IEEE International Conference on
Robotics and Automation
Pasadena, CA, USA, May 19-23, 2008

# Adaptive Grasping by Multi Fingered Hand with Tactile Sensor Based on Robust Force and Position Control

Taro Takahashi, Toshimitsu Tsuboi, Takeo Kishida, Yasunori Kawanami, Satoru Shimizu, Masatsugu Iribe †, Tetsuharu Fukushima, Masahiro Fujita

Motion Dynamics Research Group, Intelligent System Research Laboratory,
Information Technologies Laboratories, Sony Corporation
5-1-2 Kitashinagawa Shinagawa-ku, Tokyo 141-0001 Japan
[Taro.Takahashi, Toshimitsu.Tsuboi, Takeo.Kishida, Yasunori.Kawanami, Satoru.Shimizu,
Masatsugu.Iribe, Tetsuharu.Fukushima, masahirof]@jp.sony.com

*Abstract*—**In this paper we propose a new robust force and position control method for property-unknown objects grasping. The proposed control method is capable of selecting the force control or position control, and smooth and quick switching according to the amount of the external force. The proposed method was applied to adaptive grasping by three-fingered hand which has 12 DOF, and the experimental results revealed that the smooth collision process and the stable grasping is realized even if the precise surface position, the mass and the stiffness are unknown. In addition a new algorithm determines the grasp force according to the "slip" measured with the tactile sensor and the viscoelastic media on the fingertip. This algorithm works at starting and stationary state, so the friction and mass unknown object grasping is realized by the effectual force.**

## I. Introduction

With the conventional progressive researches of grasping and manipulation, we have supposed the service robot would work at home or office in the immediate future. One of the unsettled problems in this field is the property-unknown object grasping. The typical grasping strategy for property-unknown objects is (1)shape recognition by vision sensors, (2)approach with position control, (3)optimization of contact position and force and (4)grasping with force control. However, the geometrical errors result from the condition of lighting and the distance from the vision sensors. In addition, it is difficult to yield the mass, stiffness and friction of all the objects in the practical use. This paper deals with the force and position control method and adaptive grasping method.

One of the conventional approaches to force and position control is the "Hybrid Position / Force Control"[1], which is extended to the "operational space"[2]. Since the position control or the force control is selected by the "selection matrix" in these methods, it is difficult to switch each other smoothly and quickly. In the impedance control[3], the geometrical error can cause excessive force, and also the force and position control methods[1][2] have the same problem.

And some control methods of the collision process were proposed. In the method proposed in [4], using the mass-spring-damper model and linear feedback, they analyzed the stability by Lyapunov direct method. In the method proposed in [5], they use the controller including the large dumping at the collision process. However, these controllers are not designed from robustness' point of view. The force and position control based on the robust position controller[7][8] might be applied to many situations because of its robustness for the disturbance torque which becomes a problem frequently in the robot using gear drive.

In this paper we propose a new force and position control method based on the robust acceleration controller. In the proposed method, the disturbance torque (gravity, gear friction, etc.) is estimated by the disturbance observer [9] [10], whose feedback realizes the acceleration controller. And the force controller[11] is built on the acceleration controller. This controller is extended to the integrated force and position controller which has "Position Control Mode", "Force Control Mode" and "Force Constrained Position Control Mode". The third mode is capable of smooth and quick switching from the position controller into the force controller according to amount of the external force. This force controller starts working very well just after the collision. The proposed method was applied to a small multifingerd hand. The experimental results show the smooth collision process, robustness and quick response of force control. And stable grasping is realized even if precise surface positions, mass and stiffness are unknown.

At this experiment, the grasping posture and the grasping force are determined expediently. However, the more dexterous grasping will be realized in combination with various methods proposed in conventional researches, for example optimization of grasping force[12] and approach velocity[13]. We focus the slip sensing for dexterous grasping.

For the measurement of human-like tactile perception[14], the tactile sensors using the acceleration sensor[15], the "Acoustic Resonant Tensor Cell"[16], the strain gauge[17] and the Pressure-Conductive Rubber[18] were proposed. However, some of these experiments were not conducted with sensors mounted on the fingertip[15][16][17], and their margins for grasping force tend to be large [16][17][18].

We propose a new method of grasping force determination from the beginning to the stationary state by the slip, which is

† Moved to Osaka Electro-Communication University on 2007 Oct. (E-Mail: iribe@isc.osakac.ac.jp)

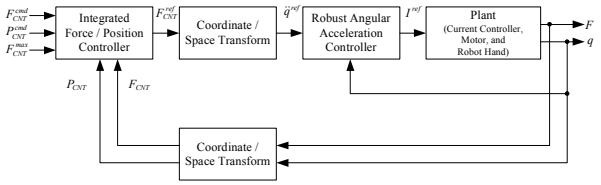


Fig. 1. The force and position controller for the adaptive grasping.

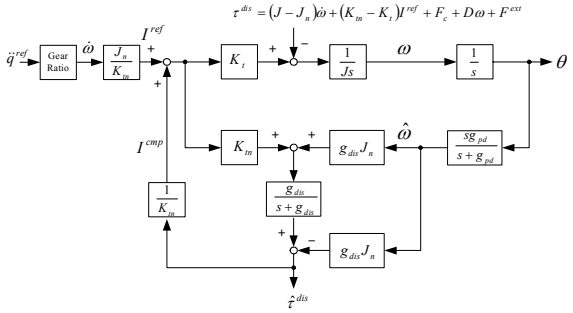


Fig. 2. Robust acceleration controller based on disturbance observer, which suppresses gravity, friction of gear and so on.

detected using the tactile sensor and the viscoelastic media on the fingertip. In the proposed method, the variable gain in force determination realizes the adaptive grasping in spite of mass and friction of the object. At stationary state, the grasping force is prevented from being too large. The effect of the proposed method was shown by experiments using a small multi-fingered hand.

## II. Robust Force and Position Control

### A. Structure of the Force and Position Robust Control

In the force and position controller for the adaptive grasping, it is desirable to design the controller so as to realize the following functions.

(a) Integrated Force and Position Control: For applications such as adaptive grasping, the position controller is useful for the approach and the force controller is useful for the grasping. In the proposed method, as in the "Hybrid Position / Force Control [1]", these controllers are selectable on each DOF (degree of freedom). In addition, one controller is able to change over another controller smoothly.

(b) External Force Limitation for Smooth Collision and Contact: The external force needs to be limited at collision and contact for stable grasping under the geometrical error. This function is realized by means of smooth and quick switching from position controller into force controller, according to the amount of the external force. In addition, it is easy to plan the grasping and the manipulation, since the external force is controlled just after the collision and the contact.

(c) Robustness of Force Control: In the assembled robot hand system, there are many factors which disturb the force control (the friction of gear, the mass of the cables, etc.). The simple modeling method of these disturbances does not make sufficient models for the computed torque method and the inverse dynamics compensation. In the proposed method, these disturbances are well compensated by the disturbance observer.

Fig. 1 shows the force and position controller for adaptive grasping. The "plant" in Fig. 1 denotes the servo motors controlled with current controller and mechanical system. The details of each block are presented in the following section.

### B. Robust Acceleration Control based on Disturbance Observer

The robust acceleration controller consists of the disturbance observer [9][10]. The total disturbance torque imposed on the system $\tau^{dis}$ is defined in (1).

$$\tau^{dis} = (J - J_n)\dot{\omega} + (K_{tn} - K_t)I^{ref} + F_c + D\omega + F^{ext} \tag{1}$$

Where $I^{ref}$ is current reference, $J$ is inertia, $K_t$ is torque coefficient, and $\omega$ is motor angular velocity. The lower suffix $n$ denotes the nominal value. The first term on the right-hand side of (1) is the self-inertia variation torque, the second term models the motor torque ripples, the third term $F_c$ is the Coulomb friction, the fourth term $D\omega$ is the viscosity friction, and the fifth term $F^{ext}$ is the reaction force.

The total calculation process of the disturbance torque estimation is shown in (2) and Fig. 2.

$$\left.\begin{aligned} \hat{\tau}^{dis} &= \frac{g_{dis}}{s+g_{dis}}(K_{tn}I_a - sJ_n\hat{\omega}) \\ &= \frac{g_{dis}}{s+g_{dis}}(K_{tn}I_a + g_{dis}J_n\hat{\omega}) - g_{dis}J_n\hat{\omega} \\ I_a &= I^{ref} + I^{cmp} \end{aligned}\right\} \tag{2}$$

where $\theta$ is the motor angle, $g_{dis}$ is the cutoff frequency of disturbance estimation, and $g_{pd}$ is the cutoff frequency of pseudo-differentiator.

Since $\tau^{dis}$ is estimated through the first-order low-pass filter, it is possible to suppress $\tau^{dis}$ in the lower band than $g_{dis}$ by the feedback of the compensation current $I^{cmp}$ determined with $\hat{\tau}^{dis}$.

$$\hat{\tau}^{dis} = \frac{g_{dis}}{s + \dfrac{K_t}{K_{tn}}g_{dis}}\tau^{dis} \tag{3}$$

$$I^{cmp} = \frac{\hat{\tau}^{dis}}{K_{tn}} \tag{4}$$

When the gain $J_n/K_{tn}$ is inserted to determine the current reference $I^{ref}$, Fig. 2 is the acceleration controller whose input is the acceleration reference.

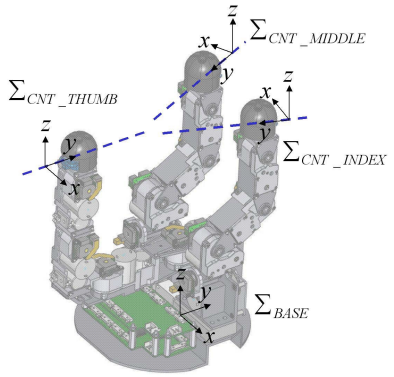


Fig. 3. The "Contact Planning Coordinate" for the grasp control.

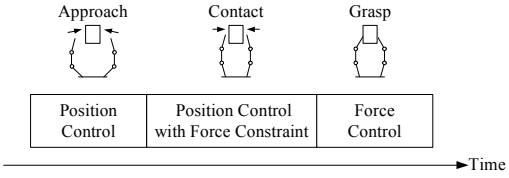


Fig. 4. Three steps in the grasping motion. The external force needs to be limited at the contact for the stable grasping under geometrical error.

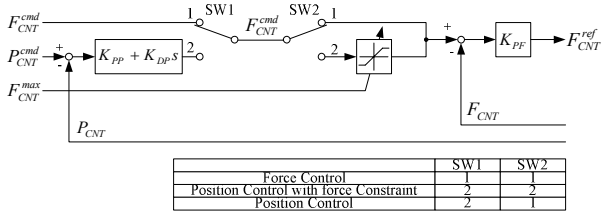


| | SW1 | SW2 |
|---|---|---|
| Force Control | 1 | 1 |
| Position Control with force Constraint | 2 | 2 |
| Position Control | 2 | 1 |

Fig. 5. The block diagram of force and position controller.

### C. Coordinate and Space Transform

Not only the base coordinate but also the additional coordinates shown in Fig. 3 are helpful to plan the grasping motion. These additional coordinates are called "Contact Planning Coordinate".

Equation (5) shows the transformation from the force reference on the contact planning coordinate $F^{ref}_{CNT}$ into the angular acceleration reference $\ddot{q}^{ref}$.

$$\ddot{q}^{ref} = \frac{1}{J_n} Jaco^{T\ BASE}T_{CNT} F^{ref}_{CNT} \tag{5}$$

where ${}^{BASE}T_{CNT}$ denotes the translation matrix from the contact planning coordinate into the base coordinate, and the force reference at the fingertip is translated into the joint torque by transpose of the Jacobian matrix $Jaco^T$. The $\ddot{q}^{ref}$ is determined with the nominal inertia $J_n$.

In the conventional approach of the force control based on the robust acceleration controller [11], the $\ddot{q}^{ref}$ is evaluated using the inverse of the Jacobian matrix $Jaco^{-1}$, which makes the controller unstable at the singular configuration. This problem can be avoided by the force-torque transform using $Jaco^T$ in the proposed method.

The coordinate transformation and the direct kinematics are employed in feedback.

### D. Integrated Position and Force Control

The grasp control consists of "Position Control Mode" for the approach, "Force Control Mode" for the grasping, and "Force Constrained Position Control Mode" for the collision and contact motion (Fig. 4). One control mode is able to change over another control mode.

In the "Force Constrained Position Control Mode", the position of the fingertip is controlled with position controller under the small external force. However, the priority of the force control is higher than the position control under the large external force in order that the external force should not go over the given "maximum external force value" $F^{max}_{CNT}$. In view of the grasp motion, it is desirable that the switching from the position control to the force control is smooth and quickly.

Fig. 5 shows the block diagram of this integrated force and position controller, which gives smooth and quick behavior in the "Force Constrained Position Control Mode". In addition this diagram realizes the mode change via SW1 and SW2 as described in the table. The values of the switch terminal 1 and 2 are cross-faded at SW1 for the purpose of the continuous reference. Equally, SW2 guaranties continuous transition between $F^{max}_{CNT}$ and $F^{cmd}_{CNT}$, and vice versa.

In the "Force Constrained Position Control Mode", the force control loop exists inside the position control loop. Since the force command $F^{cmd}_{CNT}$ generated from position control loop is limited to $F^{max}_{CNT}$, the $P^{cmd}_{CNT}$ is tracked only when the external force is smaller than $F^{max}_{CNT}$. When the external force is larger than $F^{max}_{CNT}$, $F^{cmd}_{CNT}$ becomes equal to $F^{max}_{CNT}$ and $F^{cmd}_{CNT}$ is tracked as force control. This switching is smooth because $F^{cmd}_{CNT}$ is continuous, and is quick. In the phase switching framework with event driven control[6], the "elasticity at finger tip" and "acceleration or force limitation to prevent the vibration and saturation" are mentioned as the counter measures, but they are not needed in the proposed method.

At the "Force Control Mode", the force reference $F^{ref}_{CNT}$ is calculated from the force command value $F^{cmd}_{CNT}$ and the force sensor value $F_{CNT}$.

$$F^{ref}_{CNT} = K_{PF}\left(F^{cmd}_{CNT} - F_{CNT}\right) \tag{6}$$

At the "Position Control Mode", the command value of position $P^{cmd}_{CNT}$ generates $F^{cmd}_{CNT}$, and then $F^{cmd}_{CNT}$ generates the $F^{ref}_{CNT}$.

$$F^{ref}_{CNT} = K_{PF}\left(F^{cmd}_{CNT} - F_{CNT}\right) \tag{7}$$

$$F^{cmd}_{CNT} = K_{DP}\left(K_{PP}\left(P^{cmd}_{CNT} - P_{CNT}\right) - \dot{P}_{CNT}\right) \tag{8}$$

TABLE I
SPECIFICATION OF THREE-FINGERED HAND

| | |
|---|---|
| Total Length / Finger Length (without wrist force sensor) | 191mm / 162mm |
| Weight (without wrist force sensor) | 1.0kg |
| Degree of Freedom | 12 |
| Motor Starting Torque | $8.7\times10^{-3}$ Nm, $5.6\times10^{-3}$ Nm |
| Gear Ratio | 1/94, 1/100, 1/118, 1/188 |
| Back Drivability of Planetary Gear | 0.08Nm |
| Backlash of Planetary Gear | 0.6deg |
| Rotary Encoder | 16000pulse/rev |
| Force Sensor(6 axis) | 3 (Fingertip) + 1 (wrist) |
| Tactile Sensor | 86elements, $3\times3$ mm, 38.8Hz |
| Maximum Force (Standard Posture) | 4.0N, 2.0N |
| CPU | Intel Pentium4 (3.8GHz) |
| OS | RTLinuxPro2.2 |
| Sampling Time of Controller | 0.25msec |

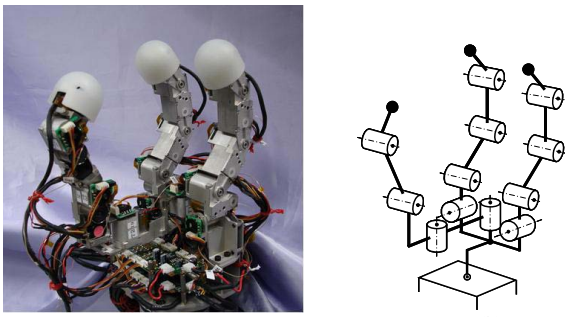

(a) (b)

Fig. 6. Three-fingered hand. (a) Appearance. (b) Configuration.

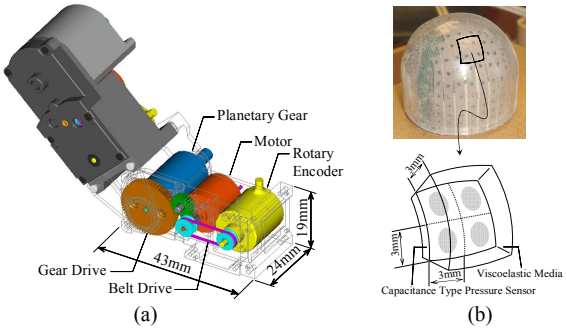


(a) (b)

Fig. 7. (a) Joint Drive Unit (b) Tactile sensor

Parallel Mild Flexion Grip Parallel Extension Grip Tip Grip

Fig. 8. Kamakura's Grasp Taxonomy

At the "Force Constrained Position Control Mode", $F_{CNT}^{cmd}$ is limited to $F_{CNT}^{max}$ so that the external force might be less than $F_{CNT}^{max}$.

$$F_{CNT}^{ref} = \begin{cases} K_{PF}\left(F_{CNT}^{cmd} - F_{CNT}\right) & if \quad \left|F_{CNT}^{cmd}\right| \le F_{CNT}^{max} \\ K_{PF}\left(F_{CNT}^{max} - F_{CNT}\right) & if \quad F_{CNT}^{cmd} > F_{CNT}^{max} \\ K_{PF}\left(-F_{CNT}^{max} - F_{CNT}\right) & if \quad F_{CNT}^{cmd} < -F_{CNT}^{max} \end{cases} \tag{9}$$

$$F_{CNT}^{cmd} = K_{DP}\left(K_{PP}\left(P_{CNT}^{cmd} - P_{CNT}\right) - \dot{P}_{CNT}\right) \tag{10}$$

When the $P_{CNT}^{cmd}$ is inside of the object surface and the finger keeps contact, $\left|F_{CNT}^{cmd}\right|$ is larger than $F_{CNT}^{max}$. So $F_{CNT}^{ref}$ is equal to $F_{CNT}^{max}$, and the external force controlled to be equal to $F_{CNT}^{max}$. The characteristics of this control are the same as "Force Control Mode".

### E. *Three-Fingered Robot Hand*

The appearance and configuration of the three-fingered hand developed for this research are shown in Fig. 6. Table I shows the specification of the hand. The total length is 191 mm, the finger length is 162 mm, and the weight is 1.0 kg. There are three fingers, and each finger has four joints. So this hand has 12 DOF, which consists of two types of small high power motor and four types of gear unit. This gear unit is composed of spur gear and planetary gear for great back drivability and strength. The planetary gear performance is shown in Table I. The small backlash especially is realized in consequence of the new planetary gear unit development.

Each joint has a 16000 pulse/rev rotary encoder, whose layout is shown in Fig. 7 (a). This parallel layout realizes the high conversion efficiency at gear unit and short length of finger.

The aims of this multi fingers hand design were maximum force, grasping posture and human-like configuration. Accordingly, the joint drive units were made up of two types of motor and four types of gear unit, considering the Kamakura's Grasp Taxonomy [19](Fig. 8). This compact multi fingered hand is capable of generating 4.0 N at the thumb fingertip and 2.0 N at the index fingertip and the middle fingertip.

The hemispherical fingertip is equipped with the 6 axis force sensor and the tactile sensor, which is capable of measuring the pressure every 3 mm at 86 points for each fingertip (Fig .7 (b)). The sampling rate of the tactile sensor is 38.8 Hz. This fingertip is covered with viscoelastic media, which was designed with the finite element method (FEM) analysis (ANSYS).

This hand is mounted on the manipulator (YASKAWA Electric Corporation, MOTOMAN-UPJ(RTLab)), which is controlled by the position controller with the disturbance observer and the vibration control. The controller for the hand and the manipulator is running on a PC with the RTLinuxPro 2.2, which outputs the current reference to the servo amplifier every sampling time 0.25 msec.

### F. *Integrated Force and Position Control Experiment*

The proposed method was applied to the "Pushing Wall" experiment. The parameter in the controller $g_{dis}$ is from 120

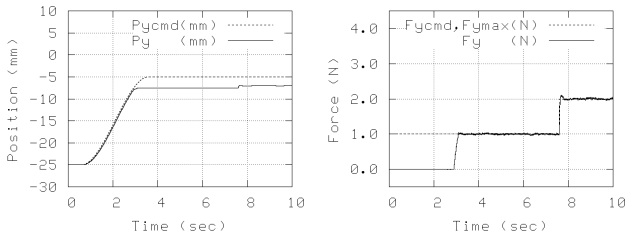


(a) Fingertip Position (b) Fingertip Force

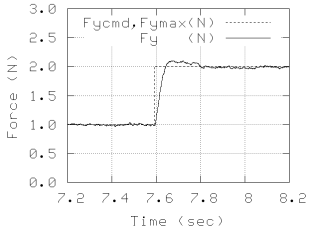


(c) Fingertip Force (Step Response)

Fig. 9. Pushing wall experiment by Proposed Method. (a)The finger started to approach at t=0.6 and went through the wall position until t=3.6. The finger collided with the wall at t=3.0, and stopped.(b) The impact force is small at the collision process (t=3.0), and the force step response (t=7.6) is excellent.(c) The time constant is 30msec.

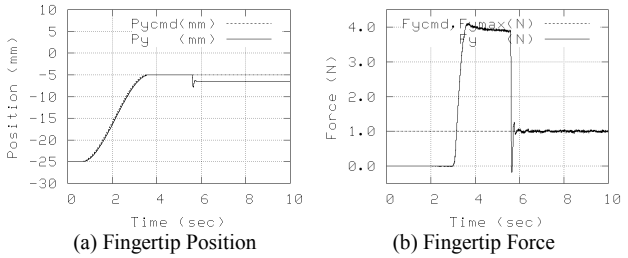


(a) Fingertip Position (b) Fingertip Force

Fig. 10. Pushing Wall Experiment by Conventional Approaches. (a)The finger collided with the wall at t=3.0 in position control. (b) Excessive contact force by the collision.

to 160 rad/sec, $K_{PP} = 50$, $K_{DP} = 30$ and $K_{PF} = 1500$. Each finger has four joints, so the controlled components are selected as $F_{CNT}^{cmd} = (f_x, f_y, f_z, m_z)$ in the thumb and $F_{CNT}^{cmd} = (f_x, f_y, f_z, m_x)$ in the index finger and middle finger. And corresponding components are selected for $P_{CNT}^{cmd}$.

Fig. 9 shows experimental results. At t=0.0sec, the thumb finger stopped at the side of the wall made by metal plate. The $P_{CNT}^{cmd}$ started to approach at t=0.6sec and went through the wall position until t=3.6sec. The finger collided with the wall and stopped at t=3.0sec. The control mode is "Position Control Mode" from t=0.0sec until t=2.0sec, "Force Constrained Position Control Mode" from t=2.0sec until t=6.0 sec, and "Force Control Mode" from t=6.0sec until t=10.0sec. Fig. 9 (b) shows that the impact force is small at the collision process (t=3.0sec). Fig. 9 (c) is the enlarged graph of the force step response (t=7.6sec), and shows quick response whose time constant is about 30msec. This is very high performance for multi joints small robot with the gear drive. And the disturbance, for example the gear friction and the gravity for frames and cables, is suppressed well. In addition, the force and the position are smooth and continuous at the mode change (t=2.0sec and t=6.0sec).

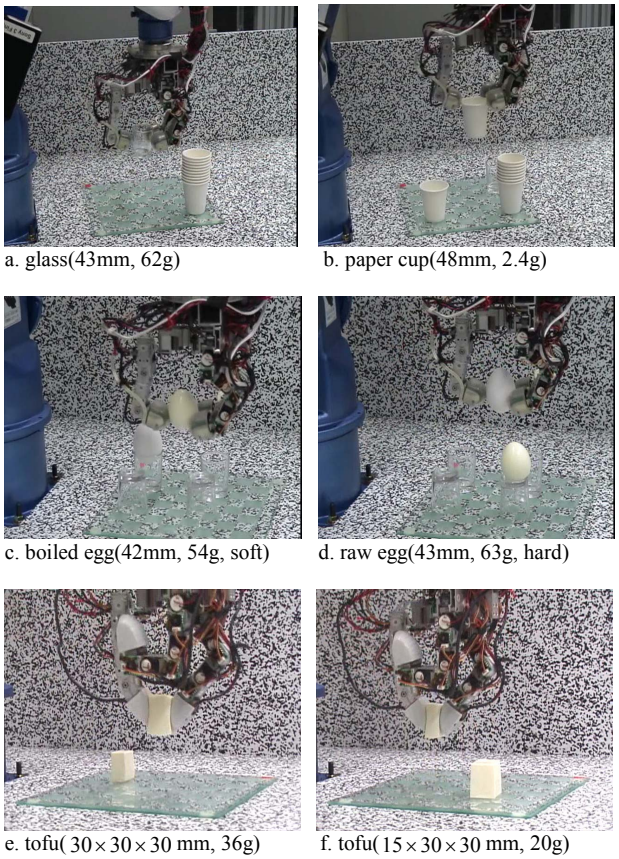

a. glass(43mm, 62g) b. paper cup(48mm, 2.4g)

c. boiled egg(42mm, 54g, soft) d. raw egg(43mm, 63g, hard)

e. tofu( $30 \times 30 \times 30$ mm, 36g) f. tofu( $15 \times 30 \times 30$ mm, 20g)

Fig. 11. Grasping of objects which are various in geometry, mass, and stiffness.

Fig. 10 shows results of a comparative experiment. In this experiment, the finger was controlled with position control while approaching and collision which is occurred by the virtual geometrical error. Fig. 10 (a) dose not show the position error since position controller is working well. However the finger configuration was bended a bit. The geometrical error causes excessive contact force shown in Fig. 10 (b). The position controller was changed to force controller at t=5.5sec.

## III. Adaptive Grasp Control

### A. Grasp Control

The proposed force and position control was applied to the "Adaptive Grasping". The "Position Control Mode" is applied for the approach and the "Force Constrained Position Control Mode" is applied for the collision and contact on the vertical axis which is illustrated with y axis in Fig. 3. For the stable grasping, the "Position Control Mode" is applied on the tangential axes which are illustrated with x and z axis. Therefore the fingertips move on the line which is parallel to vertical axis. The balanced grasping forces are decided before starting grasp in these experiments.

### B. Experimental Result of Adaptive Grasping

The proposed method was applied to the grasp control. Even if precise surface position, mass and stiffness are unknown, the proposed method makes stable grasp motion. Fig. 11 shows the grasp experiments for several kinds of objects whose size, mass and stiffness are different. While being grasped, these objects are moved by the manipulator controlled with position controller.

(a) Glass, (c) Boiled Egg without Eggshell and (d) Raw Egg are grasped with same parameter for grasp control, and contact force at thumb is 1.5 N. (b) Paper Cup is grasped with small contact force (0.25N) in order to prevent squash. Though the position of the glass was not at the set position in this experiment, the given "maximum external force" was so small (0.15N) that the finger, which collides first, kept the Glass from overturning. (e) and (f) show the grasping for various size of tofu[1] with same control parameter and same grasp force (1.0N). This tofu grasping is realized using the elliptical fingertip which is designed for compatibility between large contact area and small contact area.

## IV. Adaptive Grasp Force Control Using Tactile Sensor

Since the grasping force is determined offline, there is possibility that the properties error makes grasping failure. We propose a new algorithm for adaptive force determination with tactile sensors to avoid slipping completely.

### A. Slip Extractor using Tactile Sensor

The adaptive grasping force is determined with detected "partial incipient slippage [15][17]" in order to prevent from complete slipping. We defined this kind of slip as "values of the slip extractor" $e_x(k,N)$, which is calculated from center of pressure (COP) measured by the tactile sensors. The characteristic of the COP changes according to the contact state. Nevertheless, this kind of slip is surely detected using $e_x(k,N)$ as (11)(12).

$$e_x(k,N)=\sum_{j=1}^{2^N}K_x(j)\Delta\overline{C}_{OPx}(k,j) \tag{11}$$

$$K_x(j)=\begin{cases}C_s & if \quad \Delta\overline{C}_{OPx}<jh_{Cx}\\ C_l & if \quad \Delta\overline{C}_{OPx}\geq jh_{Cx}\end{cases} \tag{12}$$
$$\left(C_s<C_l\right)$$

where $k$ is discrete time, $\Delta\overline{C}_{OPx}(k,i)$ is amount of COP change during discrete-time interval $i$ at $k$, to which a moving average and the $3\times3$ Gaussian filter are applied. $e_x(k,N)$ is defined as the total of several $\Delta\overline{C}_{OPx}(k,i)$ to detect rapid as well as slow change of partial incipient slippage. Since $\Delta\overline{C}_{OPx}(k,j)$ is reliable when $\Delta\overline{C}_{OPx}(k,j)$ is the threshold $jh_{Cx}$ and over, the weight coefficient $K_x(i)$ is decided as (12). $e_y(k,N)$ is defined in a similar way.

[1] tofu : This Japanese tofu is the soft kind of tofu called "Silken Tofu" or "Kinugoshi Tofu (in Japanese)". This type of tofu is so soft that the "tofu steak" cannot be cooked from it.

TABLE II
PARAMETERS OF GRASP FORCE CONTROLLER

| parameter | value | parameter | value |
|---|---|---|---|
| $h_{Cx}, h_{Cy}$ | 0.1 (if N=1) | $C_s$ | 1.0 |
| $h_{Cx}, h_{Cy}$ | 0.01 (if N=2) | $Cl$ | 2.0 |
| $h_{Cx}, h_{Cy}$ | 0.005 (if N=3) | | |
| $N_f$ | 3 | $C_{sn}$ | 0.04 |
| $T_c$ | 500 | $C_{Gsn}$ | 0.015 |
| $C_{f0}$ | 2.5 | $O_{sn}$ | 0.012 |
| $C_{f1}$, $C_{f2}$ | 1.25 | $a_{sn}$ | 1000 |
| $C_{sc}$ | 0.002 | $h_{px0}$, $h_{py0}$ | 0.075 |
| $C_{Gs}$ | 0.013 | $h_{px1}$, $h_{py1}$ | 0.025 |
| $O_s$ | 2.0 | $h_{px2}$, $h_{py2}$ | 0.05 |
| $h_{slip}$ | 0.05 | $G_{px}$ | 0.15 |
| $\alpha$ | 1.5 | $G_{py}$ | 0 |

### B. Adaptive Grasp Force

The desired adaptive grasp force $F_{CNTy}^{cmd}(k)$ is determined by (13) based on $e(k,N)$ so as to prevent from complete slipping.

$$F_{CNTy}^{cmd}(k)=F_{CNTy}^{cmd}(k-1)+F_{CNTy}^{slip}(k)+F_{CNTy}^{nc}(k)+F_{CNTy}^{sp}(k) \tag{13}$$

where $F_{CNTy}^{slip}(k)$ is a term to increase the grasp force when $e(k,N)$ is large, and $F_{CNTy}^{nc}$ is a term to cancel the influence of noise in $e(k,N)$. $F_{CNTy}^{sp}$ is a term to decrease the unnecessary grasp force for holding the object.

Preliminary experiments revealed that the $e(k,N)$ became small as the normal force increased if the tangential force was constant. Consequently, $F_{CNTy}^{slip}(k)$ is decided by the product of $e(k,N)$ and normal force $f_i(k)$ as in (14)(15)(16) (17).

$$F_{CNTy}^{slip}=F_{CNTy}^{slipx}+F_{CNTy}^{slipy} \tag{14}$$

$$F_{CNTy}^{slipx}(k)=\sum_{i=0}^{N_f-1}f_i(k)G_{Sxi}(e_{Sxi}(k))e_{Sxi}(k) \tag{15}$$

$$G_{Sxi}(e_{Sxi}(k))=\frac{C_{fi}}{T_c}\left\{C_{Sc}+\frac{C_{Gs}}{1+\exp(-e_{Sxi}(k)+O_S)}\right\} \tag{16}$$

$$e_{Sx}(k)=\left|\sum_{N=1}^{3}e_x(k,N)\right| \tag{17}$$

where $N_f$ is the number of fingers, and $f_i(k)$ is measured by tactile sensors. The variable gain $G_{Sxi}$ becomes large according to $e_x(k,N)$, and is restricted within upper limit by the sigmoid function (16). $C_{Sc}$, $C_{Gs}$ and $O_S$ are parameters to shape this sigmoid function. $C_{fi}$ is weight coefficient for each finger, and $T_C$ adjusts the difference between the control cycle and the measurement cycle. The absolute value of $e_x(k,N)$ is practical so as to neglect positive and negative of

$e_x(k,N)$. $F^{slipy}_{CNTy}$ is defined in a similar way.

$e_S(k)$ has small positive value even at steady state because of white noise in $\Delta\overline{C}_{OPx}(k,i)$, and that causes increase of $F^{cmd}_{CNTy}(k)$. To cancel this increment, $F^{nc}_{CNTy}$ is defined as (18).

$$F^{ncx}_{CNTy}(k)=\begin{cases}\sum_{i=0}^{N_f-1} f_i(k)G_{Snxi}(e_{Sxi}(k))\{e_{Sxi}(k)-C_{sn}\} \\ \qquad (if \quad e_{Sxi}(k)<C_{sn}) \\ 0 \qquad\qquad (if \quad e_{Sxi}(k)\geq C_{sn})\end{cases} \tag{18}$$

$$G_{Snxi}(e_{Sxi}(k))=\frac{C_{fi}}{T_c}\left\{\frac{C_{Gsn}}{1+\exp(a_{sn}(e_{Sxi}(k)-O_{sn}))}\right\} \tag{19}$$

The absolute value of $F^{nc}_{CNTy}$ becomes small through the variable gain $G_{Snx}$ if $e_{Sx}(k)$ becomes large. $C_{Gsn}$, $a_{sn}$ and $O_{sn}$ are parameters to shape this sigmoid function. The threshold $C_{sn}$ is decided by $e_{Sx}(k)$ of stable grasp with enough force. $F^{ncy}_{CNTy}(k)$ is defined in a similar way, and $F^{nc}_{CNTy}(k)=F^{ncx}_{CNTy}(k)+F^{ncy}_{CNTy}(k)$.

$F^{sp}_{CNTy}(k)$, which suppresses excessive force for stable grasping, is defined as (20).

$$F^{sp}_{CNTy}(k)=\begin{cases}\sum_{i=0}^{N_f-1} f_i(k)\frac{C_{fi}}{T_c}\left[G_{px}\{\overline{e}_{Sxi}(k)-h_{pxi}\}+G_{py}\{\overline{e}_{Syi}(k)-h_{pyi}\}\right] \\ \qquad (if \quad \overline{e}_{Sx}<\alpha h_{px}\cap\overline{e}_{Sy}<\alpha h_{py}) \\ 0 \qquad\qquad (if \quad \overline{e}_{Sx}\geq\alpha h_{px}\cup\overline{e}_{Sy}\geq\alpha h_{py})\end{cases} \tag{20}$$

where $G_{px}$ is the gain, and $\overline{e}_{Sx}(k)$ is the moving average of $e_{Sx}(k)$. $\alpha$ must be greater than 1 for smooth change of grasp force. The threshold $h_{px}$ is decided by $\overline{e}_{Sx}(k)$ to grasp stably with small force without complete slipping. $y$ components are defined in the same way.

In addition, $F^{nc}_{CNTy}(k)$ and $F^{sp}_{CNTy}(k)$ are set to zero when $F^{slipy}_{CNTy}(k)>h_{slip}$, so that the grasping force is decreased only when the "partial incipient slippage" is small.

### C. Experimental Setup and Results

The proposed method was applied to adaptive grasping. The grasped object was a cylinder (52g) wrapped in plane paper and stuffed with additional weights (0g, 100g, 200g and 300g). The three fingers initially contact the cylinder. The thumb force is 0.3N, and the index finger and middle finger forces are decided to satisfy the equilibrium of the grasp force. $F^{cmd}_{CNTy}$ is restricted to initial grasp force and over. Table II shows parameter of proposed controller.

Fig. 12 shows experimental result of cylinder stuffed with the weight (200g). The cylinder was lifted up by manipulator at t=0.6sec, and kept at a height of 40mm between 5.6-16sec. The grasp force $F_{y0}$ is measured by 6 axis force sensor on the fingertip. Between t=0.6-2.4sec, the $F^{cmd}_{CNTy}(k)$ increase as a result of large $e_S(k)$. The $F^{cmd}_{CNTy}(k)$ decrease in consequence of small $e_S(k)$ between t=3.5-8.0sec, and is constant between t=8.0-16.0sec.

Fig. 13 shows the $F^{cmd}_{CNTy}(k)$ of experiment with weights (52g, 152g, 252g and 352g). With weight going up, the gradient of $F^{cmd}_{CNTy}(k)$ tend to be large.

Fig. 14 shows the relationship between $F^{cmd}_{CNTy}(k)$ and the mass of the object. The maximum and steady values of $F^{cmd}_{CNTy}(k)$ increase in proportion to the mass of the object. The steady value is defined as the average of $F^{cmd}_{CNTy}(k)$ from t=14sec to t=16sec, since $F^{cmd}_{CNTy}(k)$ is constant after t=14sec. The lowest force to grasp the object is proportional to its mass if its friction coefficient is constant. Therefore, the proposed adaptive grasp force is effective.

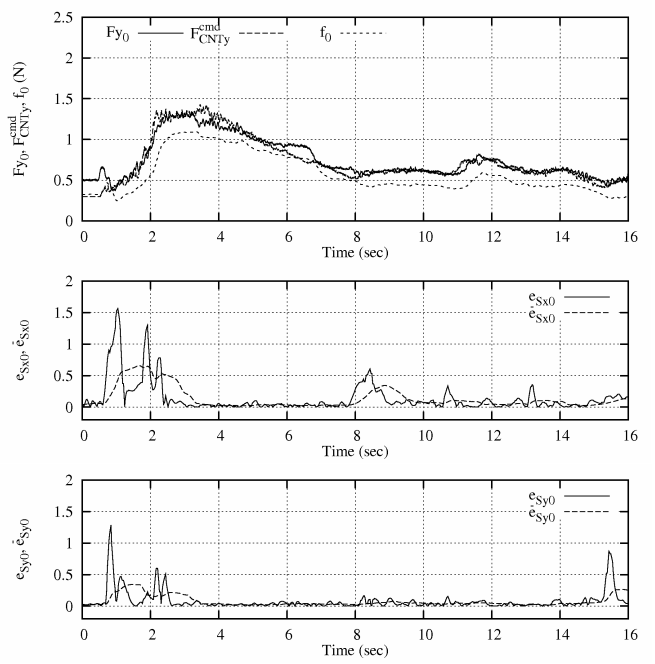


Fig. 12: Adaptive grasp force control experiment (252g)

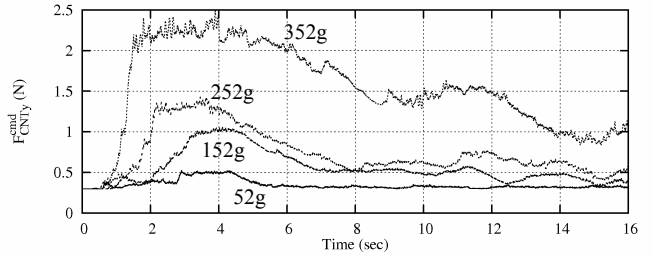


Fig. 13: Adaptive grasp force for various mass objects (52-352g)

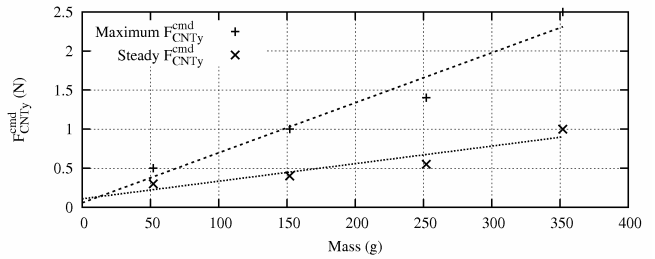


Fig. 14: Relationship between adaptive grasp force and mass of objects

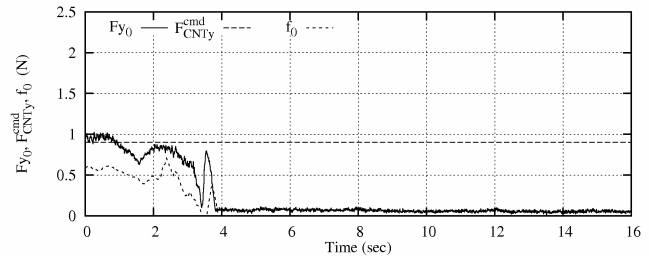


Fig.15: Slippery cube grasping with constant force (failure)

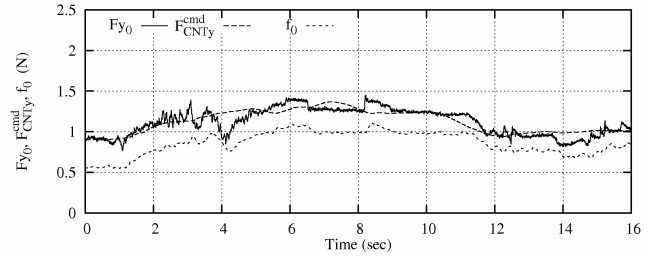


Fig.16: Slippery cube grasping with adaptive force

Not only various mass objects but also various friction objects are grasped by the proposed method. Fig. 15 shows the trial experiment of slippery cube grasping without the proposed method. This cube is dusted with powder, and its mass is 108g. The grasp force was constant(0.9N), and the grasp failed because of the cube slipperiness. Fig. 16 shows the experimental result with the proposed method. The grasping was successful because of the adaptive grasp force as is clearly shown in graph.

Although the cube(108g) is lighter than cylinder of former experiment(152g), the maximum force of slippery cube shown in Fig. 16 is larger than that of the non-slippery cylinder shown in Fig. 13. This means that the proposed method increased the grasp force enough to avoid loosing the grip on the slippery cube.

## V. CONCLUSION

In this paper we proposed the novel force and position controller for property-unknown objects grasping. The proposed method is capable of smooth and quick switching from position controller into force controller according to the amount of the external force. The experimental results on the small 12 DOF multifingered hand showed that collision process was smooth and force control response was quick (time constant is 30msec.). The proposed method realized the stable grasping for glasses, paper cups, eggs and tofu whose precise surface position, mass and stiffness were unknown. In addition a new algorithm was proposed, which determined the effectual grasping force with the tactile sensor. In the proposed method, the grasping force proportionate to mass is determined without mass-sensing, and the friction unknown object grasping was realized. The effect of the proposed method was shown by experiments using the small three-fingered hand.

## ACKNOWLEDGMENT

The authors would like to thank Dr. A. Iga, the head manager of the Information Technologies Laboratories, and all the persons concerned in this research.

## REFERENCES

[1] M.H.Raibert, John J.Craig, “Hybrid Position/ Force Control of Manipulators,” Journal of Dynamic Systems, Measurement, and Control 102, ASME, pp.126-133,1981

[2] O. Khatib, “A Unified Approach for Motion and Force Control of Robot Manipulators: The Operational Space Formulation,” IEEE Journal of Robotics and Automation, Vol.RA-3, No.1, 1987

[3] N. Hogan, “Impedance Control: An Approach to Manipulation: Part 1-3,” Journal of Dynamic Systems, Measurement, and Control 107, ASME, 1985

[4] Y. Shoji, M. Inaba, T. Fukuda, “Impact Control of Grasping,” IEEE Trans. on Industrial Electronics, Vol. 38, No. 3, pp. 187-194, 1991

[5] O. Khatib, J.Burdic, “Motion and Force Control of Robot Manipulators,” IEEE Conference on Robotics and Automation, pp.1381-1386,1986

[6] James M. Hyde and Mark R. Cutkosky, “A Phase Management Framework for Event-Driven Dextrous Manipulation,” IEEE Trans. on Robotics and Automation, Vol. 14, No. 6, pp. 978- 985, 1998

[7] Y.Hori, K.Shimura and M.Tomizuka, “Position/Force Control of Multi-Axis Robot Manipulator based on the TDOF Robust Servo Controller for Each Joint,” 11th American Control Conference, 1992

[8] K.Shimura and Y.Hori, Position, “Collision and Force Controls of Robot Manipulator based on the Robustified Joint Servosystem,” 2nd AMC Conference, 16-25, 1992

[9] K. Ohishi, K. Ohnishi, K. Miyachi, “Torque-Speed Regulation of DC Motor Based on Load Torque Estimation,” Proceedings of the IEEJ International Power Electronics Conference, IPEC-TOKYO, Vol. 2, pp. 1209-1216, 1983

[10] K. Ohnishi, M. Shibata, T. Murakami, “Motion Control for Advanced Mechatronics,” IEEE/ASME Transactions on Mechatronics, Vol. 1, No. 1, pp. 56-67, 1996

[11] T. Murakami, F. Yu, K. Ohnishi, “Torque sensorless control in multidegree-of-freedom manipulator,” IEEE Transactions on Industrial Electronics, Vol. 40, No. 2, pp. 259-265, 1993

[12] Jeffrey Kerr, Bernard Roth, “Analysis of Multifingered Hands,” International Journal of Robotics Research, Vol. 4, No. 4, pp. 3-17, 1986

[13] K. Kitagaki, M. Uchiyama, “Optimal approach velocity of end-effector to the environment,” IEEE International Conference on Robotics and Automation, vol.3, pp.1928 - 1934, 1992

[14] R. S. Johansson and G. Westling, “Roles of glabrous skin receptors and sensorimotor memory in automatic control of precision grip when lifting rougher or more slippery objects,” Experimental Brain Research 56, pp. 550-564, 1984

[15] M. R. Tremblay and M. R. Cutkosky, “Estimating Friction Using Incipient Slip Sensing During a Manipulation Task,” IEEE International conference on robotics and automation, pp.429-434, 1993

[16] T. Yoshikai, R. Tajima, S. Kagami, H. Shinoda, M. Inaba and H. Inoue, “Slip detecting by tactile sensor using Acoustic Resonant Tensor Cell and its application for grasping,” JRSJ vol. 20, No.8, pp.868-875, 2002 (in Japanese)

[17] T. Maeno, S. Hiromitsu and T. Kawai, “Control of grasping force by detecting stick/slip distribution at the curved surface of an elastic finger,” IEEE Conference on Robotics and Automation, pp. 3895-3900, 2000

[18] D. Gunj Y. Mizoguchi, A. Ming, A. Namiki, M. Ishikawa and Shimojo, "Grasping Force Control of Multi-fingered Robot Hand based on Slip Detection," Proceedings of the 2007 JSME Conference on Robotics and Mechatoronics, 1A2-B07, 2007 (in Japanese)

[19] N.Kamakura, M.Matsuo, H.Ishii, F.Mitsubosi and Y.Miura, “Patterns of static prehension in normal hands,” American Journal of Occupational Therapy, 34, 7, pp. 437-445, 1980